Podocyte Depletion Causes Glomerulosclerosis: Diphtheria Toxin–Induced Podocyte Depletion in Rats Expressing Human Diphtheria Toxin Receptor Transgene

Bryan L. Wharram,* Meera Goyal,* Jocelyn E. Wiggins,† Silja K. Sanden,* Sabiha Hussain,* Wanda E. Filipiak,§ Thomas L. Saunders,‡§ Robert C. Dysko,‖ Kenji Kohno,¶ Lawrence B. Holzman,* and Roger C. Wiggins*

*Divisions of *Nephrology, †Geriatric Medicine, and ‡Molecular Medicine and Genetics, Department of Internal Medicine, University of Michigan, Ann Arbor, Michigan; §Transgenic Animal Model Core, ‖Unit for Laboratory Animal Medicine, University of Michigan, Ann Arbor, Michigan; and ¶Research and Education Center for Genetic Information, Nara Institute of Science and Technology, Nara, Japan*

Glomerular injury and proteinuria in diabetes (types 1 and 2) and IgA nephropathy is related to the degree of podocyte depletion in humans. For determining the causal relationship between podocyte depletion and glomerulosclerosis, a transgenic rat strain in which the human diphtheria toxin receptor is specifically expressed in podocytes was developed. The rodent homologue does not act as a diphtheria toxin (DT) receptor, thereby making rodents resistant to DT. Injection of DT into transgenic rats but not wild-type rats resulted in dose-dependent podocyte depletion from glomeruli. Three stages of glomerular injury caused by podocyte depletion were identified: Stage 1, 0 to 20% depletion showed mesangial expansion, transient proteinuria and normal renal function; stage 2, 21 to 40% depletion showed mesangial expansion, capsular adhesions (synechiae), focal segmental glomerulosclerosis, mild persistent proteinuria, and normal renal function; and stage 3, >40% podocyte depletion showed segmental to global glomerulosclerosis with sustained high-grade proteinuria and reduced renal function. These pathophysiologic consequences of podocyte depletion parallel similar degrees of podocyte depletion, glomerulosclerosis, and proteinuria seen in diabetic glomerulosclerosis. This model system provides strong support for the concept that podocyte depletion could be a major mechanism driving glomerulosclerosis and progressive loss of renal function in human glomerular diseases.

J Am Soc Nephrol 16: 2941–2952, 2005. doi: 10.1681/ASN.2005010055

Glomerulosclerosis is the major pathologic process responsible for progression to ESRD in humans. Underlying conditions that predispose to glomerulosclerosis include diabetes, hypertension, IgA nephropathy, focal segmental glomerulosclerosis (FSGS), and other immune-mediated forms of glomerular injury. In aggregate, these conditions constitute 90% of end-stage kidney disease at a cost of approximately $20 billion per year in the United States (1).

Podocytes are highly differentiated neuron-like cells with limited capacity for cell division and replacement. They function to support and maintain the glomerular basement membrane filtration mechanism. Genetic mutations that result in a glomerulosclerotic phenotype occur exclusively in proteins expressed by the podocyte, thereby providing strong support for a link between podocyte dysfunction and glomerulosclerosis (2–4). Increasing evidence from experimental models suggests that podocyte loss may be a key component of the process that drives glomerulosclerosis (5–9). Data from human types 1 and 2 diabetic glomerulosclerosis and IgA nephropathy show that podocyte number is reduced in proportion to the severity of injury and degree of proteinuria (10–15). The loss of podocyte markers from glomeruli is associated with glomerulosclerosis in human biopsy samples from patients with FSGS (16,17), and increased appearance of podocytes and podocyte constituents in urine is associated with glomerulosclerosis and more rapid deterioration of renal function in FSGS, lupus nephropathy, IgA nephropathy, membranoproliferative glomerulonephritis, and diabetes (18–20). These data show a correlation between podocyte loss and glomerulosclerosis. However, whether there is a causal relationship between podocyte loss and glomerulosclerosis remains unclear. This is an important question. If podocyte depletion indeed is a universal mechanism underlying glomerulosclerosis, then this would provide a logical mechanistic explanation for the hyperfiltration hypothesis of Brenner *et al*. (21) and should also lead to a reorientation of research directed toward investigating podocyte injury leading to cell detachment and death. It would also provide an opportunity to develop valuable clinical tools to routinely monitor glomerular disease treatment strategies noninvasively by measuring podocyte products in the urine.

Received January 15, 2005. Accepted July 7, 2005.

Published online ahead of print. Publication date available at www.jasn.org.

Address correspondence to: Dr. Roger C. Wiggins, University of Michigan Health System, Division of Nephrology, Department of Internal Medicine, 1570 MSRBII, Box 0676, Ann Arbor, MI 48109-0676. Phone: 734-936-4813; Fax: 734-763-0982; E-mail: rwiggins@umich.edu.

ISSN: 1046-6673/1610-2941

To understand better the consequences of podocyte depletion for glomerular injury, we developed a model system in which the extent of podocyte loss could be regulated in adult animals with normally developed kidneys. Rodents are resistant to diphtheria toxin (DT) because rodent heparin-binding EGF-like growth factor (HB-EGF) does not bind DT. In contrast, human HB-EGF, now termed diphtheria toxin receptor (DTR; MIM number *126150), binds DT at high affinity. It serves as a shuttle that allows DT to be carried into the cell by receptor-mediated endocytosis, where it induces ADP ribosylation of polypeptide chain elongation factor 2, thus inactivating it. This results in inhibition of protein synthesis, leading to cell death (22,23). Kohno and colleagues (23) used the interspecies DTR difference and showed that the transgenic expression of human DTR (hDTR) by mouse hepatocytes allowed DT injection in transgenic (Tg) mice to cause liver-specific dose-dependent hepatotoxicity. *In vitro* studies suggest that internalization of as little as a single molecule of DT causes a cell to die (24). We chose rat (not mouse) for our model because of the widely known similarity between rat and human glomerular lesions. We showed previously that the 2.5-kb human podocin promoter drives podocyte-specific expression of LacZ in the mouse (25). We therefore used this promoter system to express hDTR specifically in rat podocytes. Injection of DT into these Tg rats caused podocyte loss in a dose-dependent manner. We used this model system to define the relationship between the extent of podocyte depletion and the development of the classical features of glomerulosclerosis, including proteinuria, mesangial expansion, adhesions of the glomerular tuft to Bowman's capsule (synechiae formation), FSGS, global sclerosis, and loss of renal function.

Materials and Methods

Tg Rats

All animal studies were approved by the University of Michigan Committee on Use and Care of Animals. Fischer 344 rats (Harlan, Indianapolis, IN) were used for these experiments because they do not develop diabetes or hypertension but do develop age-associated glomerulosclerosis (26). The hDTR cDNA was inserted 3′ of the 2.5-kb human podocin promoter (at the NcoI site of plasmid p2.5P-nlacF), which we showed previously to drive podocyte-specific LacZ expression in mice (25). The podocin promoter/hDTR Tg construct was isolated from our plasmid (p2.5P_DTR) by *Xba*I/*Hind*III restriction enzyme digestion and injected into the pronuclei of fertilized rat eggs using standard techniques. Two Tg founders were obtained, only one of which (C354) produced Tg offspring. This new Tg rat strain has been designated F344-Tg(DTR)C354Wig (RGD_ID1302921). Heterozygous offspring from this strain were used for the studies described. Tg rats were identified by PCR analysis of tail DNA using the following primer pair: 5′,5′-ACCCGACGGTCTTTAGGG-3′; 3′,5′-CCTTGTATTTC-CGAAGACATGGGT-3′. A 465-bp fragment was amplified when the transgene was present in rat genomic DNA.

Potential for DT Toxicity to Animal Handlers

As a first step in these studies, we wanted to determine what the potential risk of using DT might be for animal handlers because we were not able to establish this from the available literature. We determined by literature search that the minimum lethal dose of DT for humans is thought to be approximately 100 ng/kg body wt (27,28). All animal workers were immunized with DTP vaccine before starting these experiments and/or their anti-DT titers from previous immunizations were confirmed to be adequate. The initial animal studies were done in a biosafety level 2 animal facility with full precautions including negative pressure ventilation. Animal work was performed in a designated biosafety hood with full human protection and with all excreta collected under special precautions. Upon completion of procedures, all facilities were wiped down with 1 M NaOH to inactivate DT from inadvertent spills (28). DT activity was assessed using a CHO cell-killing bioassay system previously described and validated by Murphy *et al*. (29). Specificity was conferred by using serum from an immunized investigator (R.C.W.) to block DT cell-killing activity. We used three 100-g rats per group and collected urine and feces from these rats, which were kept in metabolic cages for 2 d before and for 3 d after intraperitoneal injection of high doses (50, 5, and 0.5 μg/kg) of DT (cat. no. D0564; Sigma, St. Louis, MO) and normal saline as a negative control. The fecal material was homogenized by Polytron (Brinkman Instruments, Westbury, NY) in PBS and centrifuged, and the supernatant was filter-sterilized through 0.45- then 0.2-μm filters. Urine samples were centrifuged and filter-sterilized through 0.2-μm filters. Serial dilutions of urine and fecal preparations were incubated with CHO cells for up to 10 d. Cell killing was measured using a 96-well plate reader (VERSAmax; Molecular Devices Corp., Sunnyvale, CA). Serially diluted DT and negative controls were run with each assay together with dilutions of antiserum previously demonstrated to block activity in the same assay and nonimmune serum as a control. Thus, for each experiment, a standard curve was generated to allow the limit of sensitivity of the assay to be determined. Assay sensitivity ranged from 3.2 to 12.8 pg of DT equivalents per well. These experiments showed that DT activity was not detected in either urine or feces ($<$15 ng/24 h DT activity in urine and $<$30 ng/24 h DT activity in feces) of 100-g rats that received doses of DT up to 50 μg/kg injected intraperitoneally. From these experiments, we determined in consultation with the University of Michigan Unit for Laboratory Animal Medicine that no special precautions were necessary for subsequent experiments involving rats that received DT doses of 50 μg/kg intraperitoneally or less. All subsequent experiments were performed in standard animal housing with no special precautions except that we diluted the DT doses in 10 ml of normal saline/100 g body wt so as to minimize the chance of significant amounts of DT being inadvertently injected into an animal handler during rat injections. In addition, all handling of DT was done in a hood by a gloved, immunized investigator, and surfaces were wiped down with 1 M NaOH after all procedures to inactivate any DT that may have inadvertently spilled.

Experimental Protocol

Rats received injections of DT diluted in 1 ml/10 g body wt normal saline or normal saline alone (as control) when they reached approximately 100 g weight. They then were kept on an *ad libitum* rat food and water diet until they were killed under anesthesia for study. For all studied rats were kept in metabolic cages, and urine was collected for 1 to 2 d before DT injection. Post-DT injection urine was collected daily for 14 d, then weekly for 2 wk (days 21 and 28). All rats were inspected daily, and if they appeared ill as judged by lethargy, ruffled fur, failure to eat or drink, they were killed before the 28-d time point (n = 15). Kidneys were perfusion-fixed using paraformaldehyde/lysine/periodate (PLP) as described previously (30). For the experiments described, 51 Tg rats were used: 10 (five male, five female) normal saline–injected controls, eight (three male, five female) receiving 10 ng/kg DT, 13 (five male, eight female) receiving 20 ng/kg DT, 18 (eight male, 10 female) receiving 50 ng/kg DT, one male rat receiving 500 ng/kg, and one male rat receiving 5000 ng/kg. There were no obvious gender differences in

response to DT noted, so data were not segregated by gender for analysis.

Protein and Creatinine Assays

Urine and serum creatinine measurements were performed using the Sigma Creatinine kit (cat. no. 555-A). For protein measurements, urine samples were precipitated with an equal volume of 30% TCA, dissolved in 1 M NaOH, then assayed using the Bio-Rad Protein Assay (cat. no. 500-0006; Hercules, CA).

Immunofluorescent and Immunoperoxidase Analysis

PLP-perfused and fixed kidney sections were embedded in paraffin. After deparaffinization and rehydration, 4-μm sections were incubated for 4 h at 92°C in Retrieve-All1 (Signet Laboratories, Dedham, MA) for antigen unmasking. For immunofluorescence studies, sections were blocked for 15 min with 10% donkey and 10% rat sera and incubated overnight at 4°C with goat anti-human HB-EGF polyclonal antibody diluted to 8.3 μg/ml (R&D Systems, Minneapolis, MN) or diluted normal goat serum as a negative control. Sections were incubated further for 3 h at room temperature with goat anti-human HB-EGF antibody and 1B4 mouse monoclonal anti-rat GLEPP1 antibody as described previously (8) or diluted normal goat serum and BB5 mouse mAb (unreactive with rat tissue) as negative controls. Sections then were incubated for 2 h at room temperature with FITC-conjugated AffiniPure donkey anti-goat IgG diluted to 7.5 μg/ml and Cy3-conjugated AffiniPure donkey anti-mouse IgG diluted to 3.75 μg/ml (Jackson ImmunoResearch Laboratories, West Grove, PA). Immunoperoxidase staining was performed using antibodies to WT1 (SC-7385 monoclonal IgG1; Santa Cruz Biotechnology, Santa Cruz, CA), nephrin (rabbit polyclonal), and GLEPP1 (1B4 monoclonal), then developed with a peroxidase system using the substrate diaminobenzidine (DAB; Vectorlabs, Burlingame, CA).

Histomorphometry

All histology was performed on PLP-perfused and fixed paraffin-embedded tissue sectioned on a Reichert-Jung 820-II microtome (Cambridge Instruments, Nussloch, Germany).

Quantification of Glomerular Tuft Adhesions. Four-micrometer sections were stained with GLEPP1 peroxidase/DAB and counterstained with periodic acid-Schiff (PAS). Results were obtained by counting at least 100 glomerular cross-sections and determining the proportion that contained adhesions of the glomerular tuft to Bowman's capsule.

Quantification of PAS-Positive Glomerular Areas. Staining was done on 4-μm sections. Podocytes were identified using peroxidase/DAB immunohistochemistry with monoclonal anti-rat GLEPP1 as primary antibody. Sections were counterstained with PAS and hematoxylin. Thus, podocytes were stained brown; nuclei were stained blue; and the remaining mesangial cells, mesangial matrix, and endothelial cells were stained pink. For each animal, consecutive glomerular cross-sections were photographed by moving systematically from outer cortex to inner cortex and back. Each glomerulus on this track without exception for 50 consecutive glomeruli was imaged. Images were collected using Spot Advanced Software (Diagnostic Instruments; Silicon Graphics, Mountain View, CA). Saved images were analyzed using the Metamorph Imaging System (Universal Imaging Corp., Downingtown, PA). The glomerular area was outlined, and the proportions of the colored glomerular tuft area that stained pink and brown were measured using the Metamorph imaging system. The hue values used were as follows: Brown 1 to 85 and pink 180 to 245. The mean value for 50 consecutive cross-sections for each animal was used for subsequent analysis.

Glomerular Volume Measurement. Glomerular tuft area data were obtained from 50 consecutive 4-μm sections stained with anti-GLEPP1 immunoperoxidase/PAS and 50 consecutive 3-μm sections stained with anti-WT1 immunoperoxidase. This information then was used to calculate average glomerular tuft volume using the Weibel formula as described previously (30), representing the mean value determined from 100 consecutive glomerular tuft cross-sections.

Podocyte Enumeration. WT1-positive nuclei were identified by immunoperoxidase staining. Number of podocytes was quantified using a modification of the thin/thick (3 μm/9 μm) section method previously described (30). Specifically, 50 consecutive glomerular cross-sections were photographed at ×200 magnification by systematically moving from superficial cortex to juxtamedullary region and back in a box pattern for 3- and 9-μm tissue sections (total 100 consecutive glomerular cross-sections). Podocytes were counted for all 100 consecutive glomerular cross-sections. Photography and morphometric analysis of the GLEPP1 peroxidase/PAS slides and podocyte counting of WT1-stained sections were performed by different individuals to provide independent measures for comparison. The values for numbers of podocytes per glomerular cross-section were used to derive a value for podocytes per tissue volume for each section thickness as described previously. The mean of the two values of podocyte number per tuft volume was then calculated. This value was divided into the value for glomerular volume calculated from measuring the area of 100 consecutive glomerular cross-sections as described in the Glomerular Volume Measurement section above. Because male and female rats have different numbers of podocytes per glomerulus and different glomerular volumes (but the same glomerular volume per podocyte), all data were expressed as percentage of normal (Tg normal saline–injected controls of the same age for each gender; $n = 5$ per gender). This allowed data from both genders to be pooled for analysis. To confirm that the podocyte counting method was reliable, we compared the podocyte counts determined by the WT1 method with an independent measurement for GLEPP1-stained area expressed as a percentage of total glomerular tuft area. As shown in the Results section, there was an excellent correlation ($r^2 = 0.87$) between these two independent methods performed by different individuals for assessing podocyte loss from glomeruli.

Results

Expression of hDTR in Podocytes of Tg Rats

Human hDTR protein was detectable at a low level in glomeruli of transgenic but not wild-type rats by immunofluorescence (Figure 1, A and B). The hDTR was distributed along the outer aspect of glomerular capillary walls, where it co-distributed with the podocyte marker GLEPP1 (Figure 1, C through E). No hDTR was seen in parietal epithelial cells of Bowman's capsule (Figure 1A). We conclude that the construct used to produce the F344 rat strain carrying the transgene (podocin promoter-driven hDTR cDNA) caused expression of hDTR in podocytes as judged by double-label immunofluorescence.

We next examined the structure of Tg rat glomeruli at the light microscopic and ultrastructural levels to determine whether expression of the transgene measurably changed glomerular structure. As shown in Figure 1, F and G, there were no detectable structural abnormalities in Tg rats. In particular, podocytes were present with a normal distribution and their foot processes were normal. Urine from Tg rats contained no

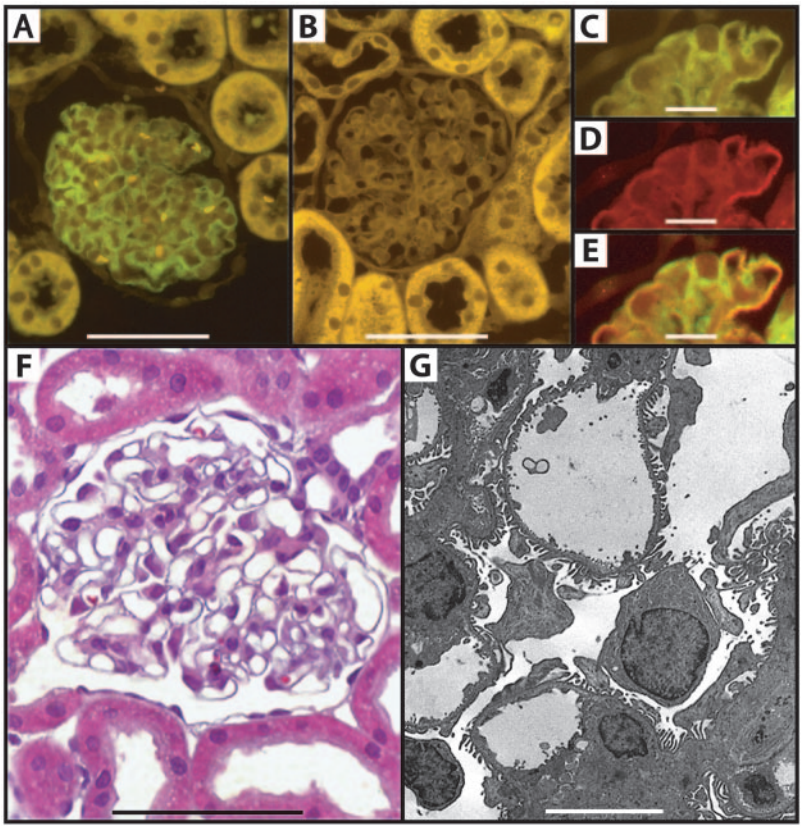

Figure 1. Podocyte-specific expression of human diphtheria toxin receptor (hDTR) in transgenic (Tg) rats. Immunofluorescent detection of human heparin-binding EGF-like growth factor (hHB-EGF; hDTR) protein was detected in glomeruli of Tg (A) but not wild-type (B) rats. hDTR was not detected in parietal (Bowman's capsule) glomerular epithelial cells (A). Double-label immunofluorescence showed that the Tg expression along glomerular capillary walls (C) was similar to the distribution of the podocyte marker GLEPP1 (D), as confirmed by the merged images (E). The histologic appearance of glomeruli from Tg rats was normal as assessed by light microscopy (F) and by electron microscopy (G). In particular, podocyte foot processes were normally distributed along the glomerular basement membrane (G). Bars = 50 μm in A, B, and F; 10 μm in C through E; and 5 μm in G.

increase in protein (data not shown). We conclude that hDTR was expressed by podocytes of Tg rats and that expression of hDTR did not change the structure and function of rat glomeruli in a detectable way as assessed by the above criteria.

Effect of DT Injection into Tg and Wild-Type Rats

DT at 50 μg/kg was injected intraperitoneally into groups of Tg and wild-type (n = 3) rat littermates. Wild-type rats showed no effect of DT injection, and urine protein excretion did not increase. In contrast, two of three Tg rats died within 10 d of DT injection, and the third seemed ill and was killed at 10 d for necropsy and analysis. At necropsy, the kidneys of Tg rats that received DT were pale and enlarged. No abnormalities were detected macroscopically in any nonrenal organs. A time course of glomerular injury was performed on additional rats that received intraperitoneal injections of 50 μg/kg DT. Histologic analysis by hematoxylin and eosin showed protein-filled tubules by day 3 and disorganized glomeruli by day 7 (Figure 2). Peroxidase staining for WT1, nephrin, and GLEPP1 showed progressive loss of these podocyte-specific markers through day 7. The urine of DT-injected Tg rats contained very high levels of protein (Figure 3A). Ultrastructural analysis (Figure 3, B through F) showed fluid-filled cysts and loss of foot processes in podocytes by day 3 (B), dense granule accumulation in podocytes by day 5 (C), and disintegration of podocytes by day 7 (D). At lower doses of DT (25 ng/kg), animals survived through day 28, at which time photomicrographs revealed glomerular basement membrane (GBM) denuded of podocytes (arrows), whereas endothelial cells (arrowheads) and mesangial cells (white asterisks) remained intact (E). We therefore conclude that we were able specifically to deplete podocytes from glomeruli of Tg rats using DT and that the time course of podocyte depletion was over 7 d for animals that received high-dose injections of DT.

Dose-Response Curve for DT in Tg Rats

We next performed studies to determine the dose response to DT (Figure 4). At DT doses >50 ng/kg, most animals died of renal failure at 10 d to 3 wk after injection. At 50 ng/kg, some rats died before the end of the 28-d observation period, but this did not occur at lower doses. Thus, we were able to cause pathologic changes in a dose-dependent manner and identified a dose range of DT for subsequent experiments.

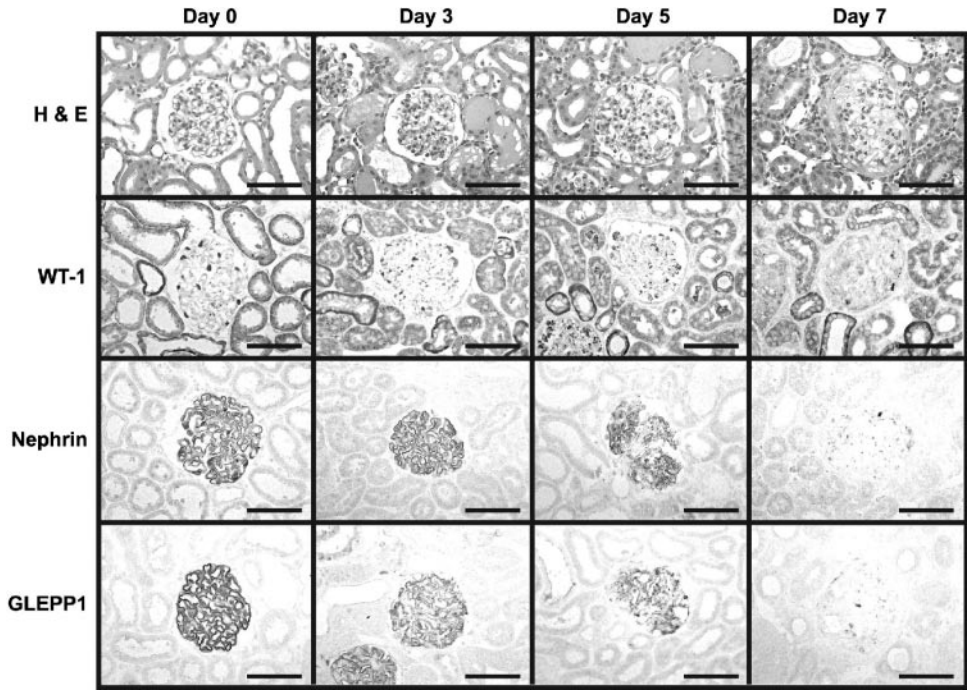

Figure 2. Podocyte depletion in Tg rats after intraperitoneal injection of 50 μg/kg DT. Photomicrographic appearance of glomeruli as assessed by hematoxylin and eosin (top) show no increase in cellularity of glomeruli, the appearance of protein in tubules by day 3, and disorganization of glomerular structure by day 7. The bottom three panel sets are immunoperoxidase/diaminobenzidine (DAB)-developed sections with antibodies to WT1 (second panel set), nephrin (third panel set), and GLEPP1 (bottom panel set) showing disappearance of WT1-positive nuclei, nephrin, and GLEPP1 proteins from glomeruli by day 7. Bars = 50 μm.

Confirmation of Podocyte-Counting Method

To evaluate whether the podocyte-counting method was reliable, we compared podocyte counts made using WT1-stained podocyte nuclei to glomerular area stained for the podocyte marker GLEPP1. GLEPP1 (also called Ptpro) is a receptor-like membrane protein tyrosine phosphatase resident on the apical surface of the podocyte that we previously cloned and characterized (31,32). It has been used as a podocyte marker by us as well as other investigators (8,16,17). The results shown in Figure 5A confirm that the WT1 podocyte-counting method shows a good correlation ($r^2 = 0.87$) with an independent measure of glomerular podocytes (proportion of glomerular tuft area that is GLEPP1 positive by immunoperoxidase). We conclude that the podocyte-counting method is satisfactory for subsequent analysis.

Podocyte Number and Glomerulosclerosis

The major features of glomerulosclerosis are mesangial matrix expansion, formation of adhesions between Bowman's capsule and the glomerular tuft (synechiae), and development of PAS-positive areas of sclerosis with collapse of glomerular capillaries. Figures 5 and 6 show that each of these features became more prominent as the extent of podocyte depletion increased. Figure 6 shows photomicrographs of glomeruli from rats that were killed 28 d after DT injection. Podocytes were stained with GLEPP1-peroxidase/DAB, and sections were counterstained with PAS and hematoxylin. Figure 5B shows that as podocyte number decreased, the glomerular PAS-positive space increased in a highly predictable way ($r^2 = 0.89$). At low-level podocyte depletion (up to 25%), there seemed to be an increase in the area stained pink with PAS (Figure 6, B and C). From Figure 6, A through C, one can see that this change seemed to be due primarily to enlargement of the mesangial area in glomerular tufts. To confirm this, we compared the percentage of the glomerular tuft area that stained pink with PAS from the normal saline–treated control rats (range for number of podocytes/glomerulus [mean $\pm$ 2 SD] was 92 to 108; $n = 10$). This group was compared with a group of rats that received DT but were still within the normal podocyte number/glomerulus range (92 to 110; $n = 5$) and a group that received DT and had a podocyte number that was just below the normal range (80 to 92; $n = 8$). The values for percentage of pink staining by PAS in these glomerular cross-sections (mean $\pm$ 1 SD) were as follows: Control 28.7 $\pm$ 3.9; DT-treated but normal podocyte number 29.9 $\pm$ 7.2; DT-treated but reduced podocyte number 37.3 $\pm$ 11.2 ($P = 0.04$ compared with the control group). Thus, we conclude that the PAS-positive glomerular space, shown in Figure 6C to be mesangial in distribution, was increased after minor loss of podocytes.

Figure 5C shows the proportion of glomeruli with adhesions to Bowman's capsule (synechiae) in relation to podocyte number. Above approximately 20% depletion, there was an increased proportion of glomeruli that contained synechiae and segmental areas of podocyte depletion and glomerulosclerosis (Figure 6, E and F). Above 40% podocyte depletion, glomeruli

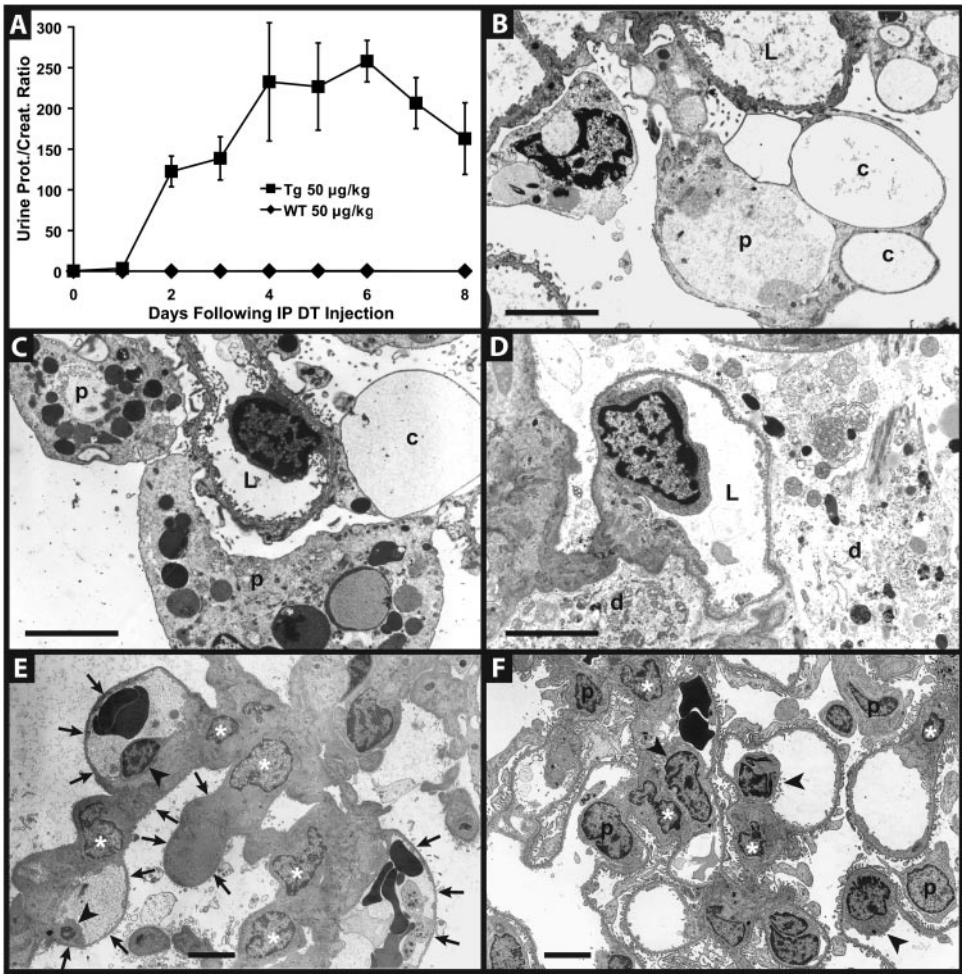

Figure 3. Podocyte depletion in Tg rats after injection of DT. (A) Intraperitoneal injection of DT at high dose (50 μg/kg) into hDTR Tg rats resulted in massive proteinuria by day 2 and peaked between 4 and 6 d after injection. The same dose had no effect on proteinuria in nontransgenic (wild-type) rats. (B through F) Ultrastructural photomicrographs of glomerular capillary loops in which the lumen (L) and podocytes (p) are identified. (B) Day 3 after DT injection. Photomicrograph showing podocytes (p) that contained fluid-filled cysts (c) and effaced foot processes. (C) Day 5 after DT injection. Photomicrograph showing podocytes (p) that contained numerous densely staining granules and effaced foot processes. (D) Day 7 after DT injection. Photomicrograph showing podocytes in the process of disintegrating (d). (E) Day 28 after lower dose (25 ng/kg) DT injection. Low-power photomicrograph showing mesangial cells (white asterisks), endothelial cells (arrowheads), and denuded glomerular basement membranes (GBM; arrows). (F) Low-power ultrastructural photomicrograph of Tg rat injected with normal saline. Mesangial cells (white asterisks), endothelial cells (arrowheads), and podocytes (p) are shown. Bars = 5 μm.

rapidly transitioned to a large proportion of glomeruli that contained synechiae (Figure 5C). At the same time, glomeruli contained larger segments of podocyte depletion and sclerosis (Figure 6, F through H). In animals with major podocyte depletion, podocytes were not detectable on tissue sections either by GLEPP1 staining (Figure 6I) or by ultrastructure (Figure 3E).

Podocyte Depletion and Proteinuria

The relationships between proteinuria and podocyte depletion, PAS-positive tuft area, and adhesions between the tuft and Bowman's capsule are shown in Figure 7. Of note, the animals seemed to segregate into two groups. Animals with a protein:creatinine ratio of <10 had less podocyte depletion, fewer synechiae, and less scarring. Those with a protein:creatinine ratio of >10 had more podocyte depletion, more synechiae, and more scarring.

Figure 8 shows the time course of proteinuria in relation to podocyte depletion. Small reductions in podocyte number (up to 20%) were associated with small transient increases in proteinuria that returned to baseline within a few days. Larger increases in podocyte depletion (21 to 40%) were associated with increased proteinuria that was still low level but persisted for the 21-d period of observation. Podocyte depletion of >40% resulted in sustained high-level proteinuria.

Podocyte Depletion and Renal Function

Serum creatinine values corrected for weight were as follows (shown as the mean ± 1 SD): Control 1.09 ± 0.20; 0 to 20%

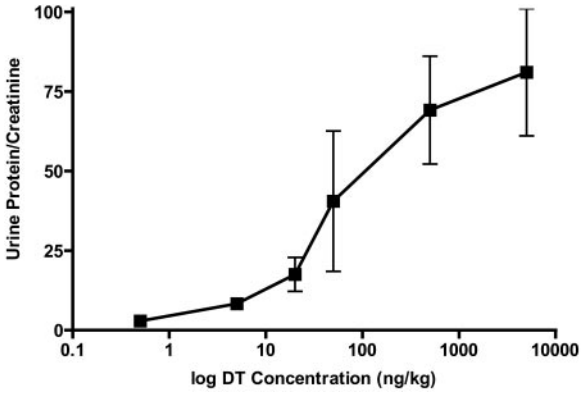

Figure 4. Dose-response curve of DT on proteinuria in Tg rats 7 d after administration of DT. The urine protein:creatinine ratio in hDTR Tg rats that received DT was dose dependent.

podocyte depletion 0.89 ± 0.18; 20 to 40% podocyte depletion 0.96 ± 0.24; >40% podocyte depletion 4.76 ± 2.56. Thus, marked podocyte depletion of >40% was required before a detectable increase in serum creatinine was present, reflecting that detectable changes in renal function are a late event in the progression of glomerular diseases.

Discussion

This report describes an experimental model wherein podocytes can be depleted from adult glomeruli at a specified time by a set amount using DT. In this model, it is likely that all podocytes that take up DT die, because a single internalized molecule of DT is thought to be able to kill a cell (24). The time course for podocyte death is approximately 7 d. In most models in which podocyte loss has been documented, the consequences of podocyte depletion are difficult to separate from other effects of podocyte dysfunction caused by diffuse podocyte injury. The specificity of this model renders it free of many of these confounding variables, allowing us to characterize the consequences of podocyte loss more definitively.

In this report, we show that the PAS-positive area of the glomerular tuft in tissue sections stained by PAS and GLEPP1 increased in association with minor loss of podocytes that caused little or no adhesion formation. This PAS-positive space is largely mesangial, as shown in Figure 6, B and C. However, at this point, we have not determined whether this represents a real increase in mesangial cell size, number, matrix, or a combination of these.

When considering the range of consequences of podocyte depletion in this model, one can divide podocyte loss into three levels of injury as shown in Table 1. Depletion of podocytes by 20% or less (stage 1) resulted in apparent mesangial expansion, transient mild proteinuria, little or no capsular adhesion formation, and no measurable change in renal function. Presumably, the remaining podocytes have the capacity to cover rapidly the denuded GBM from which podocytes have detached and can adapt to prevent both protein leakage and sclerosis from occurring. This ability to compensate for the loss of neighboring podocytes may be due in part to the expansion of the mesangial compartment as discussed below.

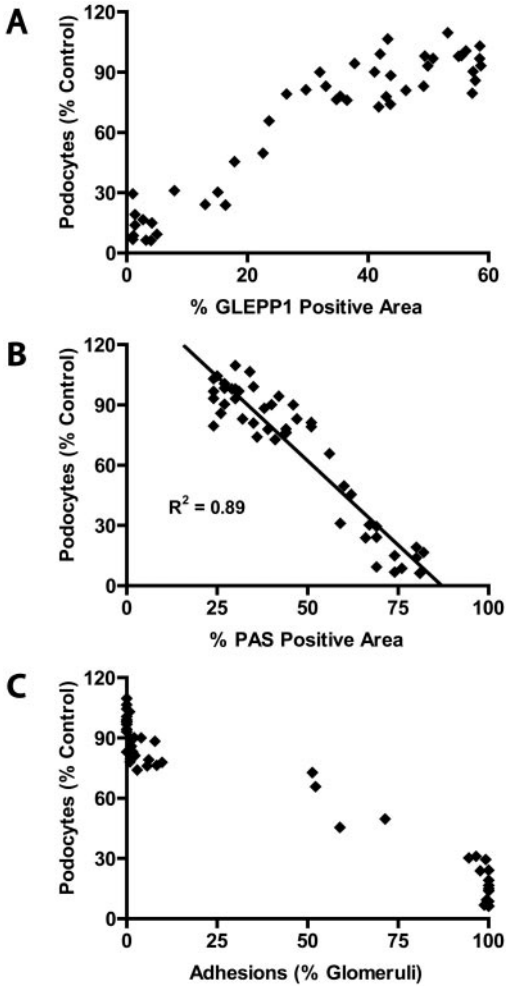

Figure 5. Effects of a reduction in podocyte number on glomerular pathology induced by varying DT dose. (A) Podocyte depletion as measured by counting WT1-positive podocyte nuclei *versus* GLEPP1-positive glomerular tuft area. A high correlation between these two independent methods of measuring podocytes was present (r^2 = 0.87). (B) Podocyte depletion was correlated directly with periodic acid-Schiff (PAS)-positive glomerular area. Note the large change in PAS-positive area associated with a small change in podocyte loss (0 to 20%). (C) Podocyte loss in relation to the proportion of glomeruli showing glomerular to capsule adhesions (synechiae). Note that with podocyte loss above approximately 20%, the proportion of glomeruli with synechiae rapidly increases so that at >40% podocyte depletion, most if not all glomeruli show synechiae.

Stage 2 (21 to 40% podocyte loss) is associated with apparent mesangial expansion, synechiae formation, FSGS, low-level but sustained proteinuria, and no detectable change in renal function. Thus, the FSGS lesions can be seen as remedial for glomeruli in that they repair (by scar formation) the injury caused by podocyte loss above a particular value. We hypothesize that the remaining podocytes cannot compensate for the GBM area exposed by 20 to 40% podocyte loss within the critical time

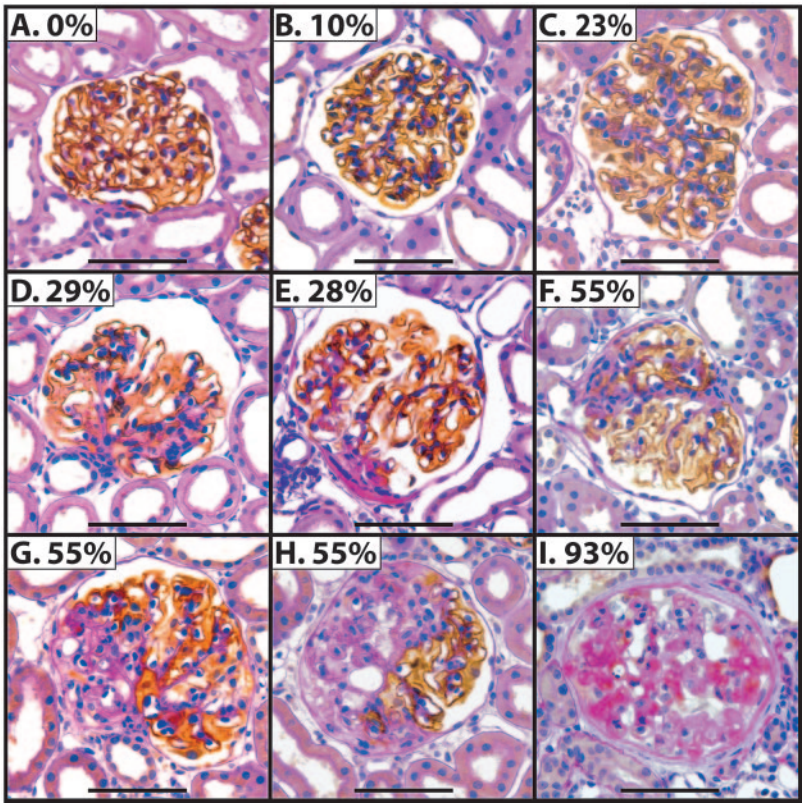

Figure 6. Photomicrographs of glomeruli from rats with increasing podocyte depletion at 28 d. Sections are stained for podocytes by immunoperoxidase anti-GLEPP1 (brown) and counterstained by PAS (pink) and hematoxylin (blue). In the box at the top left of each photomicrograph, the average proportion of podocytes depleted for that animal as counted by WT1 nuclear staining is shown. The normal small amount of pink-stained mesangial space is shown (A). As podocyte number is depleted by up to 23%, the amount of PAS-positive (pink) space increases (B and C). At 28% podocyte depletion, adhesions between the glomerular tuft and Bowman's capsule can be seen (E). With further podocyte depletion, increasingly larger segments of glomeruli are sclerotic and devoid of podocytes (F through H). With >90% podocytes depleted, some glomeruli contain no detectable podocytes and a collapsing sclerotic appearance (I). We conclude that there was a proportionate change in histologic features in relation to the proportion of podocytes lost in the model. Bars = 50 μm.

period so that scar-forming mechanisms become activated. These include adhesions between the denuded GBM and Bowman's capsule, migration of (parietal) epithelial cells from Bowman's capsule, mesangial cell division, and matrix formation as described by Kriz *et al.* (5,6).

Stage 3 occurs at podocyte depletion levels that exceed 40%. This stage is associated with a rapidly increasing proportion of glomeruli with adhesions to Bowman's capsule, an increasing proportion of glomeruli with segmental areas of podocyte loss, and glomerulosclerosis transitioning to widespread global sclerosis in animals with more podocyte depletion. Proteinuria is sustained at a high level in this group, and renal function is decreased. The data from Figure 7 showing two populations of animals with respect to proteinuria would be compatible with a self-perpetuating event taking place above the 40% podocyte depletion threshold. This type of event is also suggested by the disappearance of podocytes from whole segments of glomeruli as shown in Figure 6, F through I. Loss of podocytes from whole segments of the tuft above a particular threshold amount of podocyte loss was demonstrated previously in the puromycin aminonucleoside (PAN) model of podocyte loss in rats (8) and is similar to that seen in human biopsy material (16,17). Whiteside and colleagues (33) in 1993 described a theoretical concept whereby loss of podocytes above a threshold level would trigger widespread podocyte detachment through a receptor cooperativity model. Recent reports from Cui *et al.* (34) and Matsusaka *et al.* (35) using Tg mouse models of podocyte depletion support this concept. Loss of podocyte number above the threshold value of 40% in the rat could trigger this type of event. In both the rat and human, in which the glomerular tuft is lobulated (36), it is possible that the unraveling of podocyte detachment that occurs after a critical level of podocyte depletion could be limited to a glomerular tuft lobule. In this way, the unraveling of podocytes would be limited to a segment of a glomerulus, possibly accounting for the typical segmental appearance of many forms of progressive glomerular injury. In the mouse, the glomerular tuft anatomy seems to be simpler, so podocyte unraveling might tend to be more widespread once it was initiated. Intraglomerular hypertension could play an important role in promoting podocyte detachment and *vice versa*. Further studies will determine whether podocyte depletion *per se* causes systemic hypertension in this model.

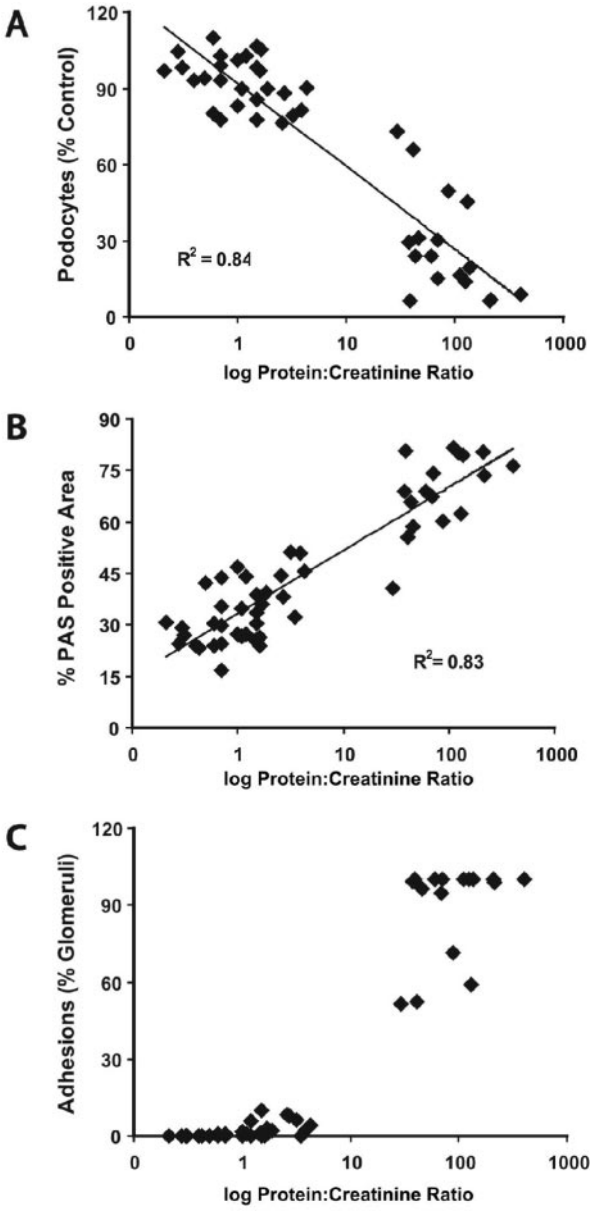

Figure 7. Relationships of proteinuria to podocyte depletion, matrix accumulation, and adhesions. (A) There was a direct correlation between podocyte depletion and proteinuria. However, the animals segregated into two obvious groups as assessed by this approach. (B) There was a direct relationship between PAS-positive glomerular area and proteinuria with two obvious groups identified. (C) There was a similar segregation of the groups when proteinuria was plotted against proportion of glomeruli with adhesions to Bowman's capsule.

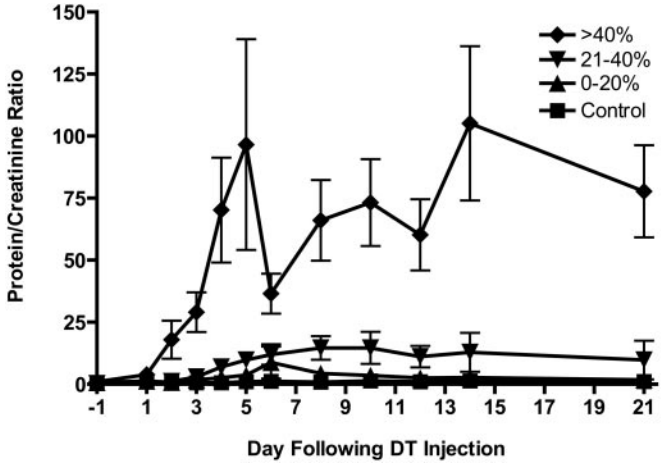

Figure 8. Time course of proteinuria according to proportion of podocytes depleted. Depletion of podocytes up to 20% resulted in a transient increase in proteinuria. Depletion of 21 to 40% of podocytes resulted in sustained low-level proteinuria. Depletion of >40% podocytes resulted in high-level sustained proteinuria.

Mesangial expansion is a central component of glomerulosclerosis and is a reason that the mesangial cell has traditionally been considered to be a likely driving factor in the development of glomerulosclerosis. We found that depletion of a relatively small number of podocytes (up to 20%) was associated with an apparent mesangial expansion. This suggests that mesangial expansion might be a downstream consequence of podocyte depletion, possibly serving as an adaptation to decrease the effective filtration surface area and thereby allow fewer podocytes to cover the active filter surface area. Mesangial expansion could occur *via* several mechanisms. A podocyte-dependent negative regulatory pathway could allow mesangial cells to replicate and/or produce matrix once podocytes have been lost, or, alternatively, a positive mesangial proliferative signal could be triggered from a glomerular cell by podocyte loss. One must also be mindful that we cannot exclude the possibility that transgene expression of hDTR by podocytes themselves could play a role in what we have observed. Rat podocytes have been reported to show increased HB-EGF protein expression after puromycin aminonucleoside injury in the rat (37). Mesangial cells have EGF receptors and produce HB-EGF, at least *in vitro* (38,39). Thus, it is possible that transgene expression of hDTR might have some impact on the model even though expression of the transgene in glomeruli was at a low level and did not itself change glomerular structure or function in a measurable way.

Can the effects of podocyte depletion seen in this model be related to human glomerular disease processes? Two excellent reports deal with podocyte depletion in type 2 diabetic glomerulonephropathy (10,14). The averaged values from these two studies for percentage of podocyte loss (relative to normal glomeruli) in individuals with type 2 diabetes and relatively normal renal function were as follows: Normalbuminuria was associated with 16% podocyte loss, microalbuminuria was associated with 24% podocyte loss, and macroalbuminuria was associated with 36% podocyte loss. These values are in the same range as those reported in this study for stages 1 and 2, indicating that the consequences of podocyte loss from the glomerulus in humans with type 2 diabetes and rats with podocyte depletion induced both in the Tg model and by PAN nephrosis are similar. Type 1 diabetic glomerulopathy and IgA nephropathy both are reported to show similar degrees of

Table 1. Stages of podocyte depletion assessed by pathologic and functional criteria[a]

Stage	Depletion	Pathology	Proteinuria	Renal Function
1	0 to 20%	Mesangial expansion[b]	Low-level transient	Normal
2	21 to 40%	Mesangial expansion,[b] adhesions, FSGS	Low-level sustained	Normal
3	>40%	Mesangial expansion,[b] adhesions, FSGS, global sclerosis	High-level sustained	Decreased

[a]FSGS, focal segmental glomerulosclerosis.
[b]Mesangial expansion indicates that this is apparent mesangial expansion on the basis of the histopathologic appearance of photomicrographs shown in Figure 6.

podocyte depletion from glomeruli in proportion to injury (12,13,15). As glomerular disease progresses in FSGS, diabetes, membranoproliferative glomerulonephritis, IgA nephropathy, and lupus nephritis, podocytes can be detected increasingly in the urine (18–20). This suggests that podocyte loss in these conditions is correlated with progression of glomerular disease. These studies of human proteinuria and kidney biopsies therefore support the concept of a direct relationship between the progression of glomerular disease and podocyte loss.

We conclude that podocyte depletion in this model causes the pathologic features commonly seen in FSGS, including apparent mesangial expansion, synechiae formation, segmental sclerosis, and global sclerosis. These events occur in proportion to the degree of podocyte depletion. Return to normal glomerular architecture over time does not occur within the time frame of our studies, unlike mesangial depletion caused by anti-Thy1 antibody (40). This probably reflects the inability of mature differentiated podocytes to replicate rapidly *in vivo* in contrast to glomerular mesangial and endothelial cells (4–6,41).

One important difference between this model and what may typically occur in humans is that in the DT model, podocytes die during a short time interval after DT injection (within approximately 7 d). In contrast, for human glomerular diseases, podocyte injury and death presumably occur over long periods of time, either intermittently or continuously. A slower podocyte depletion rate may allow greater adaptation by the remaining podocytes and other glomerular cells. In addition, the Tg rat cannot model accurately the influence of local and systemic factors such as growth factors, cytokines, and high glucose levels or hemodynamic differences associated with diabetes, hypertension, or inflammatory conditions. The differences in rate of podocyte depletion and the effects of local/systemic factors could account for the differences in glomerular structure and mesangial cell/matrix accumulation seen between this model and certain human glomerular disease states, such as diabetic glomerulosclerosis, in which nodular accumulation of mesangial matrix material is common (42).

If the features of FSGS and global sclerosis can be caused by podocyte depletion, then one is led to ask whether podocyte depletion (relative to glomerular volume or absolute) may be the single common pathologic mechanism driving the glomerulosclerosis of diabetes, hypertension, FSGS, and immune-driven glomerular diseases. We cannot at present answer that question, but we can conclude that podocyte depletion is one mechanism by which mesangial expansion, FSGS, and glomerulosclerosis can be triggered. Other possible mechanisms have not yet been separated from the podocyte depletion effect. An example that seems to be an exception to this rule is collapsing glomerulosclerosis, which occurs commonly but not exclusively in association with HIV nephropathy. However, in this condition, the visceral glomerular epithelial cells have changed their phenotype and no longer carry podocyte markers (43–45). Therefore, in this functional sense, the collapsing variant of FSGS can also be considered to be a podocyte "depletion" disease.

The concept of podocyte depletion as a major, if not universal, mechanism underlying glomerulosclerosis, perhaps in association with glomerular enlargement, is particularly important because it points to the potential clinical utility of monitoring glomerular injury by measuring podocyte products in urine. This raises the possibility of developing noninvasive methods for determining whether glomerular injury is progressing before increases in proteinuria or decreases in renal function occur. Such assays could also assess quickly the therapeutic efficacy of a given treatment regimen, allowing one to rapidly adjust therapy that is not effective without waiting for irreversible changes in function. The dream is that such assays will revolutionize our ability to prevent progression of the common renal diseases that have such high mortality rates and costs (1).

Glomerulosclerosis resulting from depletion of a highly differentiated cell type with limited capacity to replace itself (the podocyte) therefore may be a common phenotypic outcome associated with various diseases (diabetes, hypertension, FSGS, immune-mediated glomerular diseases, and genetic glomerulopathies). Other examples of diseases that stem from cell depletion include Alzheimer's disease (46), Parkinson's disease (47), Huntington's disease (48), blindness caused by loss of retinal photoreceptor cells (49), deafness caused by cochlear hair cell loss (50), and diabetes resulting from β cell depletion (51). In each case, the depletion of highly specialized "terminally differentiated" cells caused by a range of mechanisms and often superimposed on genetic susceptibilities seems to be a common pathway driving progressive organ failure. This would be in contradistinction to cell accumulation diseases, in which cells with a propensity to divide and replace themselves tend to accumulate and cause cancers. Our data support the concept that the glomeruloscleroses that are responsible for the common types of end-stage kidney diseases may also belong in this list of important cell depletion diseases.

Acknowledgments

This work was supported by grants DK46073 and P50 DK39255 from the National Institutes of Health. We gratefully acknowledge the Michigan Economic Development Corporation and the Michigan Technology Tri-Corridor for the support of this research program (Michigan Animals Model Consortium Grant 085P1000815).

We acknowledge the excellent help with tissue sectioning from Lisa Riggs. We also thank Marcus J. Moeller for helpful discussions about podocyte depletion strategies.

References

1. US Renal Data System: *USRDS 2000 Annual Data Report: Atlas of End-Stage Renal Disease in the United States*, Bethesda, National Institutes of Health, National Institute of Diabetes and Digestive and Kidney Diseases, 2000. Available: http://www.usrds.org/adr_2000.htm. Accessed August 5, 2005.
2. Asanuma K, Mundel P: The role of podocytes in glomerular pathobiology. *Clin Exp Nephrol* 7: 255–259, 2003
3. Pavenstadt H, Kriz W, Kretzler M: Cell biology of the glomerular podocyte. *Physiol Rev* 83: 253–307, 2003
4. Griffin SV, Petermann AT, Durvasula RV, Shankland SJ: Podocyte proliferation and differentiation in glomerular disease: Role of cell-cycle regulatory proteins. *Nephrol Dial Transplant* 18[Suppl 6]: vi8–vi13, 2003
5. Kriz W, Gretz N, Lemley KV: Progression of glomerular diseases: Is the podocyte the culprit? *Kidney Int* 54: 687–697, 1998
6. Kriz W: Podocyte is the major culprit accounting for the progression of chronic renal disease. *Microsc Res Tech* 57: 189–195, 2002
7. Laurens WE, Vanrenterghem YF, Steels PS, Van Damme BJ: A new single nephron model of focal and segmental glomerulosclerosis in the Munich-Wistar rat. *Kidney Int* 45: 143–149, 1994
8. Kim YH, Goyal M, Kurnit D, Wharram B, Wiggins J, Holzman L, Kershaw D, Wiggins R: Podocyte depletion and glomerulosclerosis have a direct relationship in the PAN-treated rat. *Kidney Int* 60: 957–968, 2001
9. Schiffer M, Bitzer M, Roberts IS, Kopp JB, ten Dijke P, Mundel P, Bottinger EP: Apoptosis in podocytes induced by TGF-beta and Smad7. *J Clin Invest* 108: 807–816, 2001
10. Pagtalunan ME, Miller PL, Jumping-Eagle S, Nelson RG, Myers BD, Rennke H, Coplon N, Sun L, Meyer TW: Podocyte loss and progressive glomerular injury in type II diabetes. *J Clin Invest* 99: 342–348, 1997
11. Meyer TW, Bennett PH, Nelson RG: Podocyte number predicts long-term urinary albumin excretion in Pima Indians with type II diabetes and microalbuminuria. *Diabetologia* 42: 1341–1344, 1999
12. Steffes MW, Schmidt D, McCrery R, Basgen JM: International Diabetic Nephropathy Study Group: Glomerular cell number in normal subjects and in type I diabetic patients. *Kidney Int* 59: 2104–2113, 2001
13. White KE, Bilous RW, Marshall SM, El Nahas M, Remuzzi G, Piras G, De Cosmo S, Viberti G; the European Study for the Prevention of Renal Disease in Type I diabetes (ESPRIT): Podocyte number in normotensive type I diabetic patients with albuminuria. *Diabetes* 51: 3083–3089, 2002
14. Dalla Vestra M, Masiero A, Roiter AM, Saller A, Crepaldi G, Fioretto P: Is podocyte injury relevant in diabetic nephropathy? Studies in patients with type 2 diabetes. *Diabetes* 52: 1031–1035, 2003
15. Lemley KV, Lafayette RA, Safai M, Derby G, Blouch K, Squarer A, Myers BD: Podocytopenia and disease severity in IgA nephropathy. *Kidney Int* 61: 1475–1485, 2002
16. Sharif K, Goyal M, Kershaw D, Kunkel R, Wiggins R: Podocyte phenotypes as defined by expression and distribution of GLEPP1 in the developing glomerulus and in nephrotic glomeruli from MCD, CNSF, and FSGS. A dedifferentiation hypothesis for the nephrotic syndrome. *Exp Nephrol* 6: 234–244, 1998
17. Barisoni L, Kriz W, Mundel P, D'Agati V: The dysregulated podocyte phenotype: A novel concept in the pathogenesis of collapsing idiopathic focal segmental glomerulosclerosis and HIV-associated nephropathy. *J Am Soc Nephrol* 10: 51–61, 1999
18. Hara M, Yanagihara T, Kihara I: Urinary podocytes in primary focal segmental glomerulosclerosis. *Nephron* 89: 342–347, 2001
19. Kanno K, Kawachi H, Uchida Y, Hara M, Shimizu F, Uchiyama M: Urinary sediment podocalyxin in children with glomerular diseases. *Nephron Clin Pract* 95: c91–c99, 2003
20. Vogelmann SU, Nelson WJ, Myers BD, Lemley KV: Urinary excretion of viable podocytes in health and renal disease. *Am J Physiol Renal Physiol* 285: F40–F48, 2003
21. Brenner BM, Lawler EV, Mackenzie HS: The hyperfiltration theory: A paradigm shift in nephrology. *Kidney Int* 49: 1774–1777, 1996
22. Mitamura T, Higashiyama S, Taniguchi N, Klagsbrun M, Mekada E: Diphtheria toxin binds to the epidermal growth factor (EGF)-like domain of human heparin-binding EGF-like growth factor/diphtheria toxin receptor and inhibits specifically its mitogenic activity. *J Biol Chem* 270: 1015–1019, 1995
23. Saito M, Iwawaki T, Taya C, Yonekawa H, Noda M, Inui Y, Mekada E, Kimata Y, Tsuro A, Kohno K: Diphtheria toxin receptor-mediated conditional and targeted cell ablation in transgenic mice. *Nat Biotechnol* 19: 746–750, 2001
24. Yamaizumi M, Mekada E, Uchida T, Okada Y: One molecule of diphtheria toxin fragment A introduced into a cell can kill the cell. *Cell* 15: 245–250, 1978
25. Moeller M, Sanden S, Soofi A, Wiggins R, Holzman L: Two gene fragments that direct podocyte-specific expression in transgenic mice. *J Am Soc Nephrol* 13: 1561–1567, 2002
26. Yu BP, Masoro EJ, McMahon CA: Nutritional influences on aging of Fischer 344 rats: I. Physical, metabolic, and longevity characteristics. *J Gerentol* 40: 657–670, 1985
27. Pappenheimer AM Jr: The story of a toxic protein, 1888–1992. *Protein Sci* 2: 292–298, 1993
28. Environmental Control and Research Program, Division of Safety, National Institutes of Health: Diphtheria toxin Safety Data Sheet, 1998. Available: http://www.niehs.nih.gov/odhsb/datasheets/pdf/diphtheria_toxin.pdf. Accessed August 5, 2005.
29. Murphy JR, Bacha P, Teng M: Determination of Corynebacterium diphtheriae toxigenicity by a colorimetric tissue culture assay. *J Clin Microbiol* 7: 91–96, 1978
30. Sanden SK, Wiggins JE, Goyal M, Riggs LK, Wiggins RC: Evaluation of a thick and thin section method for estimation of podocyte number, glomerular volume and glomerular volume per podocyte in rat kidney with Wilms' tu-

mor-1 protein used as a podocyte nuclear marker. *J Am Soc Nephrol* 14: 2484–2493, 2003
31. Thomas PE, Wharram BL, Goyal M, Wiggins JE, Holzman LB, Wiggins RC: GLEPP1, a renal glomerular epithelial cell (podocyte) membrane protein-tyrosine phosphatase. Identification, molecular cloning, and characterization in rabbit. *J Biol Chem* 269: 19953–19962, 1994
32. Wiggins RC, Wiggins JE, Goyal M, Wharram BL, Thomas PE: Molecular cloning of cDNAs encoding human GLEPP1, a membrane protein tyrosine phosphatase: Characterization of the GLEPP1 protein distribution in human kidney and assignment of the GLEPP1 gene to human chromosome 12p12–p13. *Genomics* 27: 174–181, 1995
33. Cho CR, Lumsden CJ, Whiteside CI: Epithelial cell detachment in the nephritic glomerulus: A receptor co-operativity model. *J Theor Biol* 160: 407–426, 1993
34. Cui S, Guo G, Li C, Willecke K, Quaggin SE: Innocent bystander theory for progression to glomerulosclerosis in a transgenic mouse model [Abstract]. *J Am Soc Nephrol* 15: 241A, 2004
35. Matsusaka T, Xin J, Niwa S, Kobayashi K, Akatsuka A, Hashizume H, Wang QC, Pastan I, Fogo AB, Ichikawa I: Genetic engineering of glomerular sclerosis in the mouse via control of onset and severity of podocyte-specific injury. *J Am Soc Nephrol* 16: 1013–1023, 2005
36. Venkatachalam M, Kritz W: Anatomy. In: *Heptinstall's Pathology of the Kidney*, 5th Ed., edited by Jeanette JC, Olson JL, Schwartz MM, Silva FG, Philadelphia, Lippincott-Raven, 1998, pp 3–66
37. Khong TF, Fraser S, Katerelos M, Paizis K, Hill PA, Power DA: Inhibition of heparin- binding epidermal growth factor-like growth factor increases albuminuria in puromycin aminonucleoside nephrosis. *Kidney Int* 58: 1098–1107, 2000
38. Takemura T, Murata Y, Hino S, Okada M, Yanagida H, Ikeda M, Yoshioka K: Heparin-binding EGF-like growth factor is expressed by mesangial cells and is involved in mesangial proliferation in glomerulonephritis. *J Pathol* 189: 431–438, 1999
39. Mishra R, Leahy P, Simonson MS: Gene expression profiling reveals role for EGF-family ligands in mesangial cell proliferation. *Am J Physiol Renal Physiol* 283: F1151–F1159, 2002
40. Shankland SJ, Hugo C, Coats SR, Nangaku M, Pichler RH, Gordon KL, Pippin J, Roberts JM, Couser WG, Johnson RJ: Changes in cell-cycle protein expression during experimental mesangial proliferative glomerulonephritis. *Kidney Int* 50: 1230–1239, 1996
41. Pabst R, Sterzel RB: Cell renewal of glomerular cell types in normal rats. An autoradiographic analysis. *Kidney Int* 24: 626–631, 1983
42. Olson JL: Diabetes Mellitus. In: *Heptinstall's Pathology of the Kidney*, 5th Ed., edited by Jeanette JC, Olson JL, Schwartz MM, Silva FG, Philadelphia, Lippincott-Raven, 1998, pp 1247–1286
43. Meyrier A: E pluribus unum: The riddle of focal segmental glomerulosclerosis. *Semin Nephrol* 23: 135–140, 2003
44. Barisoni L, Kopp JB: Modulation of podocyte phenotype in collapsing glomerulopathies. *Microsc Res Tech* 57: 254–262, 2002
45. Yang Y, Gubler MC, Beaufils H: Dysregulation of podocyte phenotype in idiopathic collapsing glomerulopathy and HIV-associated nephropathy. *Nephron* 91: 416–423, 2002
46. Dickson DW: Apoptotic mechanisms in Alzheimer neurofibrillary degeneration: Cause or effect? *J Clin Invest* 114: 23–27, 2004
47. Tatton WG, Chalmers-Redman R, Brown D, Tatton N: Apoptosis in Parkinson's disease: Signals for neuronal degradation. *Ann Neurol* 53[Suppl 3]: S61–S70, 2003
48. Heinsen H, Strik M, Bauer M, Luther K, Ulmar G, Gangnus D, Jungkunz G, Eisenmenger W, Gotz M: Cortical and striatal neurone number in Huntington's disease. *Acta Neuropathol* 88: 320–333, 1994
49. Lev S: Molecular aspects of retinal degenerative diseases. *Cell Mol Neurobiol* 21: 575–589, 2001
50. Minoda R, Izumikawa M, Kawamoto K, Raphael Y: Strategies for replacing lost cochlear hair cells. *Neuroreport* 15: 1089–1092, 2004
51. Gale EA: Molecular mechanisms of beta-cell destruction in IDDM: the role of nicotinamide. *Horm Res* 45[Suppl 1]: 39–43, 1996

See related editorial, "Role of Podocytes in Focal Sclerosis: Defining the Point of No Return," on pages 2830–2832.